RSC Advances

A graphic abstract

Pd nanoparticles decorated on different graphene supports have been prepared by a gas-liquid interfacial plasma method. The hybrid materials have been used to catalyze Heck coupling reactions and Pd nanoparticles decorated oxidized graphene foam (Pd/OGF) is found to be the most active catalyst. More importantly, the Pd/OGF catalyst has been successfully used for one-pot synthesis of dibenzyls with different aryl bromides and olefins.

Journal Name

ARTICLE

Plasma synthesis of oxidized graphene foam supporting Pd nanoparticles as a new catalyst for one-pot synthesis of dibenzyls

Liang Ren,[‡a] Fan Yang,[‡a] Chunxia Wang,[b] Yongfeng Li,[a]* Hailing Liu,[a] Zhiqiang Tu,[a] Liqiang Zhang,[a] Zhichang Liu,[a] Jinsen Gao[a] and Chunming Xu[a]

We have developed an environmentally-friendly method to the synthesis of Pd nanoparticles (Pd NPs) decorated different graphene supporters, and the morphology and structure of hybrids are characterized by transmission electron microscopy, X-ray diffraction, X-ray photoelectron spectroscopy and elemental mappings. Four hybrid materials based on graphene foam (GF), oxidized graphene foam (OGF), graphene oxide (GO) and reduced graphene oxide (RGO) have been used to catalyze Heck coupling reactions, and the effect of supporter on the activity of the hybrid material has been studied. Our results have revealed that Pd NPs decorated OGF (Pd/OGF) is the most active catalyst, showing better performance than the commercial Pd/C catalyst. More importantly, Pd/OGF catalyst has been successfully used for one-pot synthesis of dibenzyls with different aryl bromides and olefins, which has simplified the separation and purification process and realized the green organic synthesis.

Introduction

Graphene is a two-dimensional material of sp^2-hybridized carbon. Due to its extraordinary electronic, mechanical, and chemical properties, graphene has attracted much interest in both theoretical and experimental studies.[1] Graphene can be used as an excellent catalyst supporter due to its large surface area and high thermal, chemical and mechanical stability.[2] Additionally, metal nanoparticles have many applications in catalysis, electronics and optics due to their excellent properties.[3] Therefore, graphene supported metal nanoparticles can combine the advantages of graphene and metal nanoparticles, which has recently drawn much attention.[4] There are many approaches to the synthesis of hybrid materials combining metal nanoparticles and graphene, including gas-phase reduction, hydrothermal method, microwave assisted reduction, chemical reduction and plasma reduction.[2h, 5] Among these methods, the gas-liquid interfacial plasma (GLIP) method has many advantages such as ultra-high density, high reactivity, high process rate, preparation of nanomaterials in large scale, avoiding use of toxic stabilizers and reducing agents, the continuous synthesis, reaction at ambient temperature, and no need to stir during the nanoparticle formation process.[6]

In the field of heterogeneous catalysis, palladium catalyzed C-C cross coupling reactions have great significance due to its industrial potential for the synthesis of chemicals and their intermediates.[2e] Heck reaction is one of the most important cross coupling reactions, which is the most powerful and widely used method to couple aryl halides and olefin compounds.[7] Moreover, the products of Heck reactions have extensive applications as intermediates in the preparation of chemical products, pharmaceutical products and bioactive compounds.[8] Dibenzyls (the hydrogenation products of stilbenes) can be used to form important substructures of several natural and synthetic compounds such as lunularic acid, an antifungal agent, bifluranol and flame retardants.[9] Compared with synthesis of dibenzyls by two steps, one-pot synthetic approach can minimize the separation and refining of intermediates. The synthesis of dibenzyls in one-pot has been previously reported,[10] but the current methods exhibit some limitations, such as harsh reaction conditions, complex in catalyst preparation and device manufacturing.

In this work, we have performed a green GLIP method to homogeneously deposit Pd NPs on different kinds of graphene. The effect of four kinds of graphene supporters on the deposition of Pd NPs has been investigated. The four hybrid materials have been used to catalyze Heck reactions, and our findings demonstrate that Pd/OGF shows the best catalytic performance compared with other graphene-based catalysts. Furthermore, Pd/OGF catalyst has been successfully used for one-pot synthesis of dibenzyls, which reduces the separation and purification process of the intermediate compounds and realizes the green organic synthesis.

Experimental section

[a]State Key Laboratory of Heavy oil Processing, China University of Petroleum, Changping 102249, Beijing, China. Fax: +86-10-89739028; Tel: +86-10-89739028; E-mail: yfli@cup.edu.cn

[b]Beijing National Laboratory for Molecular Sciences, Key Laboratory of Analytical Chemistry for Living Biosystems, Institute of Chemistry, the Chinese Academy of Science, Beijing 100190, China

‡ These authors contributed equally.

† Electronic supplementary information (ESI) available: ^{1}H NMR data for products in Table 4

Materials

All chemicals received were used without further purification: 4-Bromoanisole, N-methyl-2-pyrrolidone (NMP), 1-Butyl-3-methylimidazolium Tetrafluoroborate ([BMIM]BF$_4$) and Palladium 10% on Carbon (Aladdin industrial corporation); Palladium acetate, Bromobenzene, 4-Bromoacetophenone and Styrene (Tokyo Chemical Co., Ltd > 40%); 4-Bromotoluene, 4-Bromochlorobenzene, Ethyl acrylate, Caesium carbonate and Triethylamine (J&K Scientific Co., Ltd); Ethanol, Methanol, Toluene, Potassium carbonate, Sodium acetate, Sodium borohydride, Sulfuric acid, Phosphoric acid, Hydrochloric acid, Hydrogen peroxide, Ferric trichloride, Potassium permanganate, Anhydrous magnesium sulfate, Petroleum ether and Ethyl acetate (Beijing chemical works).

Fabrication of four kinds of graphene

GF was grown on the 1.7-mm-thick nickel foam (12×12 cm square plates) by a CVD method[11] in a 4-inch chamber quartz reactor under following conditions: argon flowing at 300 sccm/min, the temperature at 940 °C, atmospheric pressure and the flow ration of CH$_4$:H$_2$ at 10:30 for 20 min. Then the nickel foam was corroded in the mixed solution of FeCl$_3$ and HCl (0.5 mol/L FeCl$_3$, 5 v% HCl). The resulting suspension was filtered and washed by deionized water and EtOH for several times, and then the solid was vacuum-dried to obtain the final product.

OGF was synthesised according to the improved Hummers' method.[12] A 9:1 mixture of concentrated H$_2$SO$_4$/H$_3$PO$_4$ (20:2 mL) was added to a mixture of GF (150 mg, 1 wt. equiv.) and KMnO$_4$ (900 mg, 6 wt. equiv.), producing a slight exotherm to 35-40 °C. The reaction was then heated to 50 °C and stirred for 12 h. The reaction was cooled to room temperature and poured onto ice (~300 mL) with 30 wt. % H$_2$O$_2$ (1 mL). A yellow suspension was obtained and washed repeatedly with deionized water to remove the remaining salt until the PH reached about 7 and then dialyzed for one week. After centrifugation, the sediment was redispersed in 400 mL deionized water and sonicated for 3 hours, and then the suspension was dried through the rotary evaporation apparatus.

The synthesis process of GO is similar to that used for the OGF, but using the graphite powder as a raw material.

RGO was prepared by chemical reduction method.[13] GO (100 mg) was dispersed in deionized water (100 mL) and sonicated for 1 h, and then NaBH$_4$ (400 mg) was added to the dispersion. The mixture was stirred for 30 min and heated at 125 °C for 3 h. The yellow-brown solution gradually yielded a black precipitate during the reduction process. The black solid was isolated by centrifugation, washed with deionized water and finally dried.

Fabrication of Pd NPs decorated four kinds of graphene

The hybrid materials of Pd NPs decorated different kinds of graphene were prepared by a GLIP method at ambient temperature for 10 min.[4e] The glow plasma was generated between the top flat stainless steel (SUS) and bottom ionic liquid electrode. Ar gas was introduced and used as the plasma-forming gas. V_{DC} = 200-240 V was applied to a stainless steel electrode in gas phase for the generation of an Ar plasma, where the discharge current I was fixed to 0.02 A and the Ar gas was introduced up to a pressure of 180 Pa. 48 mg GF, OGF, RGO, GO were added to the reactor and 11.2 mg Pd(OAc)$_2$ was dispersed in [BMIM]BF$_4$ (Pd/G [graphene] weight ratios 1:9). Then the Pd solution was added to the reactor and the mixture

of Pd solution and graphene was left for 10 min. For the formation of Pd NPs, electrons were irradiated toward the ionic liquid for 10 min, then the mixture was sonicated in ethanol to remove the excess impurities and extracted from the ionic liquid by a centrifuge process. The hybrid materials of Pd NPs decorated different graphene supports were prepared, and the respective materials were called Pd/GF, Pd/OGF, Pd/RGO and Pd/GO.

General procedure for Heck reactions

Different catalysts corresponding to a percentage of palladium of 1 mol% with respect to aryl halides were used during the reaction process. 0.1 mmol of aryl halides and 0.12 mmol of olefin were mixed together in a pressure vial, after that 0.12 mmol K$_2$CO$_3$ and 0.3 mL NMP were added in the solution, then the mixture was stirred at 130 °C. The reaction process was monitored by the thin-layer chromatography (TLC). After completion of the reaction, the mixture was cooled to room temperature and filtered. The filtrate was diluted with 20 mL H$_2$O, followed by extraction three times (2 × 15 mL) with ethyl acetate. The organic phase was dried over MgSO$_4$, filtered and dried through the rotary evaporation apparatus. The mixture was then purified by silica gel column chromatography using ethyl acetate and petroleum ether as eluents.

Pd/OGF catalyzed hydrogenation reactions of stilbenes

1-methoxy-4-styrylbenzene (21 mg, 0.1 mmol), Pd/OGF (1.53 mg, 1mol% Pd) and EtOH (2 mL) were placed together in a pressure vial, then the mixture was stirred at 60 °C under a H$_2$ atmosphere (1 atm). The reaction process was monitored by the TLC. After completion of the reaction, the mixture was purified as mentioned above to obtain the product.

Pd/OGF catalyzed the reaction of one-pot synthesis of dibenzyls

0.1 mmol of aryl halides, 0.12 mmol of olefin, 0.12 mmol of K$_2$CO$_3$ and 0.3 mL NMP were mixed together in a pressure vial. The amount of Pd/OGF catalyst used in each reaction was 1.53 mg (1 mol% Pd), and the reaction mixture was stirred at 130 °C. The reaction process was monitored by the TLC. After completion of Heck reaction, the mixture was cooled to 60 °C, and 1.7 mL EtOH was added, then the mixture was stirred at 60 °C under a H$_2$ atmosphere (1 atm). Upon completion of the reaction, the mixture was purified as mentioned above to gain the product. The product identification was conducted by ^{1}H NMR measurement on a Bruker DMX-300 spectrometer using CDCl$_3$ as a solvent.

Characterization of graphene supports and the catalyst

Transmission electron microscopy (TEM, Tecnai G2, F20) combined with elemental mappings at an acceleration voltage of 200 kV was used to measure the morphology, size distribution and element composition of samples. X-ray diffraction (XRD, Bruker D8 Advance Germany) was applied to characterize the crystal structure of the hybrid materials, and the data were collected on a Shimadzu XD-3A diffractometer using Cu Kα radiation. The X-ray photoelectron spectroscopy (XPS, Thermo Fisher K-Alpha American with an Al K α X-ray source) was used to measure the elemental composition of samples. The Pd NPs amounts of different Pd/G hybrid materials were determined by an inductively coupled plasma optical emission spectrometer (ICP-OES).

Results and discussion

Characterization of graphene supporters and Pd/G hybrid materials

In order to synthesise the Pd/G hybrid materials, different graphene supporters have been first prepared. The SEM and TEM images of different graphene supporters are displayed in Fig. 1. The SEM image of GF is shown in Fig. 1a which indicates that the prepared GF has three-dimensional interconnected structure and the pore size distributes in the range of 300-500 μm. Before the oxidation, the TEM image in Fig. 1b reveals that GF have clear cut hexagonal crystalline with 7 layers (the layer number of most GF is from 5 to 10) compared with that after oxidation shown in Fig. 1c, in which the structure of graphene has been destroyed and the defects appear. Fig. 1d shows the low-magnification TEM image of GO, showing that GO has flake structure. In contrast to GF, GO and RGO have many defects, as shown in Figs. 1e, 1f.
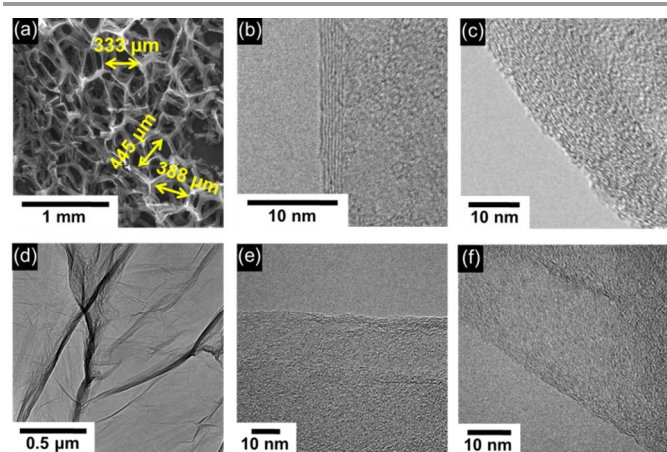

Fig. 1 SEM image of GF (a); High resolution TEM images of GF (b), OGF (c), low resolution TEM image of GO (d), high resolution TEM images of GO (e), RGO (f).

In addition, the XPS spectra of GF, OGF, GO and RGO are compared in Fig. 2 and the high-resolution XPS spectrum for C1s of GF, OGF, GO and RGO are shown in Fig. S1. The oxygen content of GF is 5.2 wt% which is mainly due to the adsorption from air, while the oxygen content of OGF is 36.5 wt%, implying that the oxidation process of GF is successful. Also, the oxygen content of GO is 34.0 wt%, demonstrating that the preparation of GO has been achieved. In comparison, the oxygen content of RGO is 14.8 wt%, showing that the part of oxygen-containing groups have been effectively removed during $NaBH_4$ reduction.
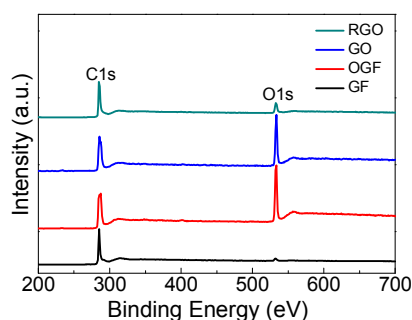

Fig. 2 XPS spectra of GF, OGF, GO and RGO.

The TEM images of different Pd/G hybrid materials are shown in Figs. 3a-d. The corresponding Pd nanoparticle size and loading content of Pd/G are summarized in Figs. 3e-f. According to the TEM images, it is found that the GLIP method is efficient for the preparation of the Pd/G hybrid materials. The results demonstrate that all synthesized Pd NPs on graphene supporters exhibit uniform morphologies and the particle diameters for Pd/GF, Pd/OGF, Pd/RGO and Pd/GO are in the range of 4.0-6.5 nm. It is worthy to mention that the high-density Pd deposition has been achieved and the Pd loading amounts for Pd/GF, Pd/OGF, Pd/RGO and Pd/GO are in the range of 4.5-7.0 wt. % which is checked by ICP-OES. Specially, the largest loading amount of Pd NPs is up to 6.91 wt. % for Pd/OGF, showing homogeneous distribution of Pd NPs with the very small size 4.8 nm.
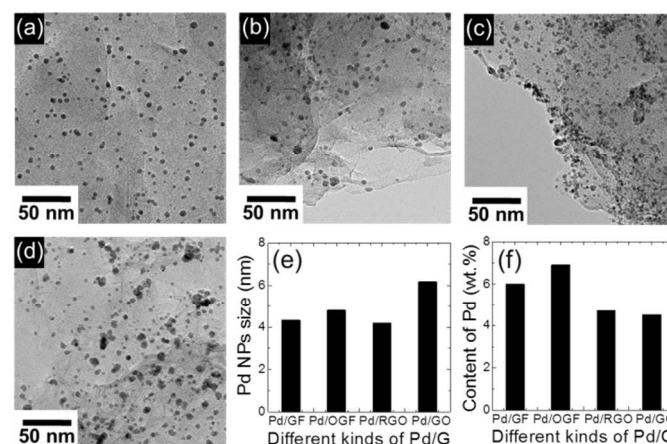

Fig. 3 TEM images of Pd/GF (a), Pd/OGF (b), Pd/RGO (c) and Pd/GO (d); Pd nanoparticle size of different kinds of Pd/G (e), Pd content of different kinds of Pd/G (f).
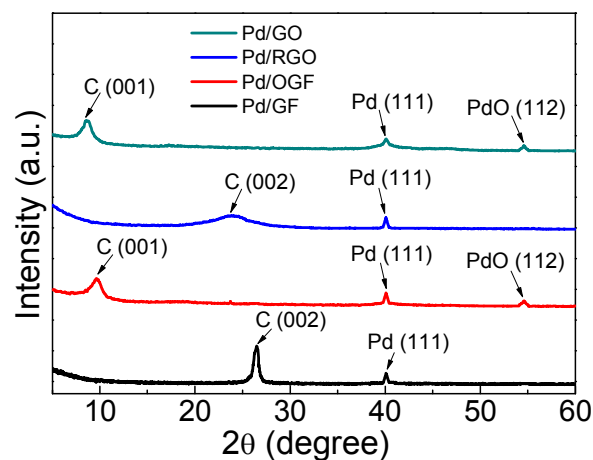

Fig. 4 XRD spectra of Pd/GF, Pd/OGF, Pd/RGO and Pd/GO.

Moreover, XRD spectra of different kinds of Pd/G are indicated in Fig. 4. For Pd/GF, the characteristic diffraction peaks are observed at 26.5° and 40.1°, which can be attributed to (002) crystal plane of graphene and (111) crystal plane of Pd(0).[14] For Pd/OGF, the characteristic peaks are detected at 9.6°, 40.1° and 54.6°, which corresponds to (001) crystal face of OGF, (111) crystal face of Pd(0) and (112) crystal face of PdO.[15] For Pd/RGO, the characteristic peaks are found at 23.7° and 40.1°, which can be associated with (002) crystal plane of

graphene and (111) crystal plane of Pd(0). It is interesting to note that the (002) crystal plane of graphene for Pd/RGO is less than 26.5° because RGO has some oxygen species which can be inserted into the graphene layers and cause the increase of the crystal plane spacing. For Pd/GO, the characteristic peaks are found at 8.6°, 40.1° and 54.6°, which corresponds to (001) crystal face of GO, (111) crystal face of Pd(0) and (112) crystal face of PdO. The results demonstrate that oxidized graphene supporters are beneficial to generate crystal planes of PdO.

The XPS spectroscopy has been used to check the chemical composition and chemical bonds of each element in the samples. Fig. 5a demonstrates the XPS spectra of Pd/GF, Pd/OGF, Pd/RGO and Pd/GO, indicating that the main chemical components are C 1s, O 1s and Pd 3d in the samples, and the high-resolution XPS spectrum for C1s of Pd/GF, Pd/OGF, Pd/RGO and Pd/GO are shown in Fig. S2. The enlarged image of Pd 3d for the four samples is shown in the inset of Fig. 5a, from which we can find that there are four peaks (Pd $3d_{5/2}$, PdO $3d_{5/2}$, Pd $3d_{3/2}$, PdO $3d_{3/2}$) for Pd/OGF and Pd/GO, while there are only two peaks (Pd $3d_{5/2}$, Pd $3d_{3/2}$) for Pd/GF and Pd/RGO. The above results reveal that PdO species are easily generated in the oxidized graphene supporters. The C 1s XPS spectrum is split into four functional groups, including a C-C bond at 284.7 eV, a C-O bond at 285.3 eV, a C=O bond at 286.7 eV and an O-C=O bond at 287.4 eV, as indicated in Fig. 5b. Fig. 5c shows the high-resolution XPS spectrum for O 1s which is divided into three components, a C=O bond at 531.4 eV, an O-H bond at 532.3 eV and a C-O bond at 533.1 eV. Fig. 5d demonstrates the high-resolution XPS spectrum for Pd 3d in which there are four types of Pd structure in Pd/OGF. Pd $3d_{5/2}$ (335.7 eV) and Pd $3d_{3/2}$ (341.0 eV) indicates the presence of Pd(0) in the sample, while PdO $3d_{5/2}$ (338.0 eV) and PdO $3d_{3/2}$ (343.2 eV) reveals the presence of Pd(II) in the sample.

Fig.6 HAADF-STEM images (a), and elemental mappings (b-d) of Pd/OGF.

General procedure for Heck reactions

It is well known that Pd-catalyzed Heck reactions are of significant importance in fine chemical synthesis. The effect of experimental conditions on Heck reaction has been studied and the results are summarized in Table 1. The influence of base on the Heck reaction is first studied. The reaction of 4-bromoanisole with styrene has been performed in the presence of 1 mol% Pd/GF as a catalyst and NMP as a solvent under N_2 atmosphere, and different bases are used (Table 1, entries 1-5). It is found that K_2CO_3 worked the best compared with other bases. Then, the influence of concentration of substrate is investigated with the optimized base. 0.1 mmol 4-bromoanisole and 0.12 mmol styrene are performed with different contents of NMP (Table 1, entries 5-7). The results demonstrate that the concentration of substrate has an important effect on the Heck reaction, and 0.333 mol/L is found to be the best. Moreover, the effect of catalysts-based on different graphene supporters on the Heck reaction is examined with the optimized base and concentration of substrate (Table 1, entry 5 and entries 8-10). According to the results, it can be concluded that Pd/OGF is the best catalyst for the reaction with yield up to 95%, which is much more active than the commercial Pd/C catalyst (Table 1, entry 11). Furthermore, the product yield is only 19% (Table 1, entry 12) using Pd particles as a catalyst, much lower than the four hybrid materials, mainly due to the serious aggregation of Pd nanoparticles, as shown in Fig. S3. Importantly, the catalysts based on the oxidized graphene supporters are found to have higher catalytic activity because there are highly active PdO

have been carried out during TEM measurements. Fig. 6a shows the high-angle annular dark-field scanning transmission electron microscopy (HAADF-STEM) image for the mapping area, and the elemental mappings of C, O, Pd are presented in Figs. 6b-d. Three elements of carbon, oxygen and palladium are well dispersed in the sample, and the content of these three elements is gradually reduced. The well dispersed palladium active species may play an important role for the catalytic reaction.
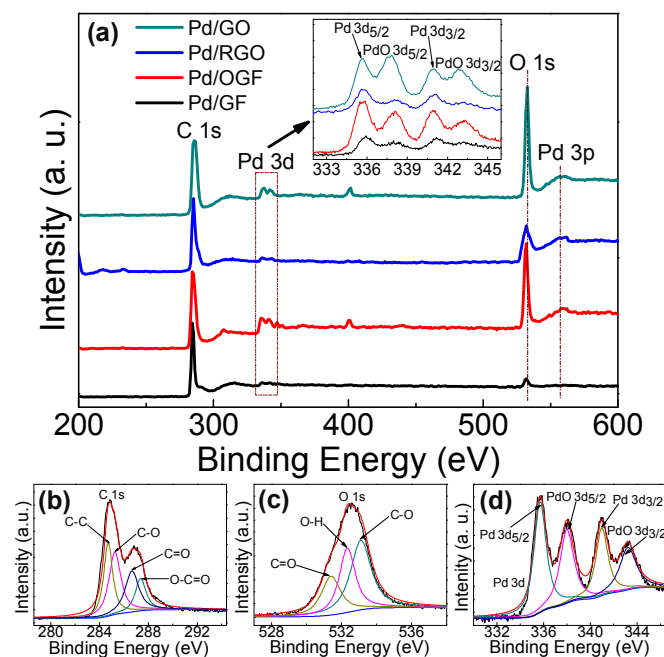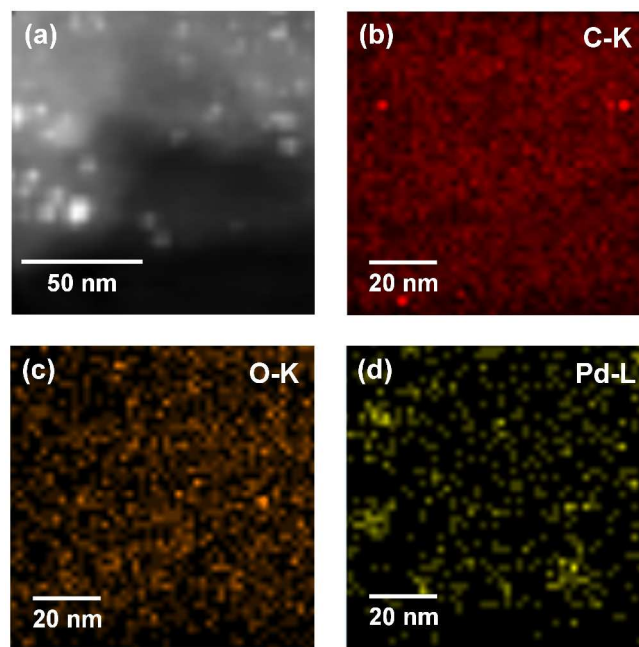

Fig. 5 XPS spectra of (a) Pd/GF, Pd/OGF, Pd/RGO and Pd/GO; High-resolution XPS spectra of C 1s (b), O 1s (c) and Pd 3d (d) of Pd/OGF.

In order to obtain direct evidences of the elemental composition and distribution, elemental mappings of Pd/OGF

species on the oxidized graphene supporters.[16] In addition, the catalytic activity of Pd/OGF is found to be higher than Pd/GO. This is because that Pd/OGF has smaller Pd NPs size since OGF has larger surface area than GO due to its macroporous structure, which can supply more active sites for adsorption of Pd NPs. The reusability of Pd/OGF is not satisfied due to the aggregation of Pd NPs (supporting information).

Table 1. Effect of different conditions on Heck coupling reaction[a]
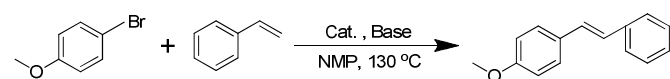
Entry	Base	Conc. (mol/L)	Cat.	Yield[b] (%)
1	none	0.333	Pd/GF	trace
2	Et$_3$N	0.333	Pd/GF	84
3	NaOAc	0.333	Pd/GF	41
4	Cs$_2$CO$_3$	0.333	Pd/GF	23
5	K$_2$CO$_3$	0.333	Pd/GF	88
6	K$_2$CO$_3$	0.167	Pd/GF	14
7	K$_2$CO$_3$	0.5	Pd/GF	85
8	K$_2$CO$_3$	0.333	Pd/OGF	95
9	K$_2$CO$_3$	0.333	Pd/RGO	59
10	K$_2$CO$_3$	0.333	Pd/GO	71
11	K$_2$CO$_3$	0.333	Pd/C	48
12	K$_2$CO$_3$	0.333	Pd NPs	19

[a] Reaction conditions: 4-Bromoanisole (0.1 mmol), Styrene (0.12 mmol), base (0.12 mmol), NMP, cat. (1 mol%), 130 °C, 15 h, under N$_2$. [b] Isolated yield.

Furthermore, the scope of the high reactivity of Pd/OGF catalyzed Heck coupling reactions has been also examined and the results are summarized in Table 2. The reaction of bromobenzene and styrene has been carried out in the presence of 1 mol% Pd/OGF, 0.12 mmol K$_2$CO$_3$ and 0.3 mL NMP, giving the desired product yield with 96% in 6 h at 130 °C (Table 2, entry 1). To achieve similar product yield, longer reaction times have been observed for 4-bromotoluene and 4-bromoanisole (Table 2, entries 2 and 3), while shorter reaction times have been used for 4-bromochlorobenzene and 4-bromoacetophenone (Table 2, entries 4 and 5). The results demonstrate that electron-withdrawing substituents promote the coupling reaction, while electron-donating groups have a negative effect on the reaction. Moreover, the excellent yield is also obtained with the reaction of 4-bromoacetophenone and ethyl acrylate (Table 2, entry 6).

Table 2 Heck coupling reactions of aryl halide with olefin[a]
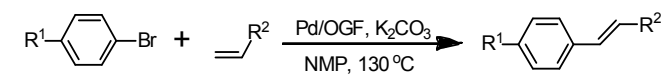
Entry	R^1	R^2	Time (h)	Yield[b] (%)
1	4-H	Ph	6	96
2	4-CH$_3$	Ph	6	96
3	4-OCH$_3$	Ph	15	95
4	4-Cl	Ph	3	96
5	4-COCH$_3$	Ph	3	95
6	4-COCH$_3$	CO$_2$Et	3	96

[a] Reaction conditions: Aryl halide (0.1 mmol), Olefin (0.12 mmol), K$_2$CO$_3$ (0.12 mmol), NMP (0.3 mL), cat. (Pd/OGF, 1 mol%), 130 °C, under N$_2$. [b] Isolated yield.

Pd/OGF catalyzed hydrogenation reactions of stilbenes

Moreover, we have examined the Pd/OGF catalyzed hydrogenation reactions of stilbenes (the products of Heck

reactions). First, the influence of solvent on the hydrogenation reaction is shown in Table 3. The hydrogenation reaction of 1-methoxy-4-styrylbenzene has been performed in the presence of 1 mol% Pd/OGF as a catalyst under 1 atm pressure of H$_2$ at room temperature, and different solvents are used (Table 3, entries 1-5). The results demonstrate that EtOH is the best solvent compared with other solvents, and the desired product yield is up to 100%. The effect of temperature on the hydrogenation reaction has been investigated with the optimized solvent. The product yield at 60 °C is 100% in contrast to the yield of 94% at room temperature; therefore, 60 °C is the best temperature for the reaction.

Table 3. Effect of different solvents on hydrogenation reaction[a]
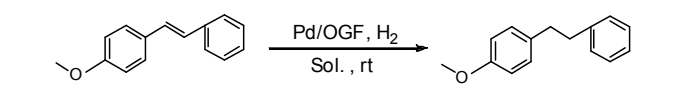
Entry	Solvent	Time (h)	Yield[b] (%)
1	H$_2$O	20	trace
2	MeOH	14	94
3	EtOH	14	100
4	Toluene	20	trace
5	NMP	20	85

[a] Reaction conditions: 1-methoxy-4-styrylbenzene (0.1mmol), solvent (2 mL), cat. (Pd/OGF, 1 mol%), rt, 1 atm H$_2$. [b] Isolated yield.

Pd/OGF catalyzed the reaction of one-pot synthesis of dibenzyls

Based on the above results, one-pot synthesis of dibenzyls has been tried in our work, and the results are shown in Table 4. The process of one-pot synthesis is as follows: the reaction of 0.1 mmol aryl halide and 0.12 mmol olefin has been first proceeded with the presence of 1 mol% Pd/OGF, 0.12 mmol K$_2$CO$_3$ and 0.3 mL NMP at 130 °C under N$_2$ atmosphere, then the product is added 1.7 mL EtOH and continued to react under atmosphere pressure of H$_2$ at 60°C, and the final product is isolated by silica gel column chromatography to calculate the yield and checked by ^{1}H NMR (supporting information). Different aryl bromides and styrene give the desired product yield from 86% to 89% (Table 4, entries 1-5). Compared with the report by Djakovitch et al.,[10a] our method has offered milder reaction conditions for one-pot synthesis of dibenzyls. Moreover, the high yield up to 89% is also achieved with the reaction of 4-bromoacetophenone and ethyl acrylate (Table 4, entry 6). The results confirm that the route of one-pot synthesis is successful.

Table 4 One-pot synthesis reactions of aryl halide with olefin[a]
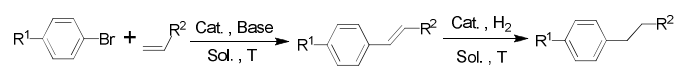
Entry	R^1	R^2	Time (h)		Yield[b] (%)
			t_1	t_2	
1	4-H	Ph	6	12	88
2	4-CH$_3$	Ph	6	12	88
3	4-OCH$_3$	Ph	15	12	86
4	4-Cl	Ph	3	12	89
5	4-COCH$_3$	Ph	3	12	87
6	4-COCH$_3$	CO$_2$Et	3	8	89

[a] Reaction conditions: Aryl halide (0.1 mmol), Olefin (0.12 mmol), K$_2$CO$_3$ (0.12 mmol), cat. (Pd/OGF, 1 mol%), solvent (first step: NMP 0.3mL, second step: EtOH 1.7 mL), temperature (first step: 130 °C, second step: 60 °C). [b] Isolated yield.

Conclusions

In conclusion, we provide an environmentally-friendly method to prepare four different kinds of Pd/G hybrids, Pd/GF, Pd/OGF, Pd/RGO and Pd/GO. The different Pd/G hybrids have been characterized by TEM, XRD and XPS. The results demonstrate that Pd/GF and Pd/OGF have smaller Pd NPs sizes and higher Pd loading amount than Pd/RGO and Pd/GO, and oxidized graphene supporters are beneficial to generate highly active PdO. These four hybrid materials have been used to catalyze Heck reactions, and the results indicate Pd/OGF is the most active catalyst. This catalyst has also been successfully applied to catalyze the hydrogenation reaction of 1-methoxy-4-styrylbenzene under mild conditions. Furthermore, Pd/OGF catalyst has been used for the reaction of one-pot synthesis of dibenzyls with different aryl bromides and olefins, and the results demonstrate that the product yield is higher than 85%. The route of one-pot synthesis has simplified the separation and purification process and realized the green organic synthesis. Further work is in progress to extend this catalyst for new organic molecular transformations.

Acknowledgements

Notes and references

1. (a) J. C. Meyer, A. K. Geim, M. I. Katsnelson, K. S. Novoselov, T. J. Booth and S. Roth, *Nature*, 2007, **446**, 60; (b) L. A. Ponomarenko, F. Schedin, M. I. Katsnelson, R. Yang, E. W. Hill, K. S. Novoselov and A. K. Geim, *Science*, 2008, **320**, 356; (c) K. S. Novoselov, Z. Jiang, Y. Zhang, S. V. Morozov, H. L. Stormer, U. Zeitler, J. C. Maan, G. S. Boebinger, P. Kim and A. K. Geim, *Science*, 2007, **315**, 1379; (d) K. S. Novoselov, A. K. Geim, S. V. Morozov, D. Jiang, Y. Zhang, S. V. Dubonos, I. V. Grigorieva and A. A. Firsov, *Science*, 2004, **306**, 666; (e) A. K. Geim and K. S. Novoselov, *Nat. Mater.*, 2007, **6**, 183; (f) C. Lee, X. D. Wei, J. W. Kysar and J. Hone, *Science*, 2008, **321**, 385.

2. (a) P. V. Kamat, *J. Phys. Chem. Lett.*, 2010, **1**, 520; (b) Y. C. Si and E. T. Samulski, *Chem. Mater.*, 2008, **20**, 6792; (c) H. M. A. Hassan, V. Abdelsayed, A. Khder, K. M. AbouZeid, J. Terner, M. S. El-Shall, S. I. Al-Resayes and A. A. El-Azhary, *J. Mater. Chem.*, 2009, **19**, 3832; (d) G. Goncalves, P. Marques, C. M. Granadeiro, H. I. S. Nogueira, M. K. Singh and J. Gracio, *Chem. Mater.*, 2009, **21**, 4796; (e) G. M. Scheuermann, L. Rumi, P. Steurer, W. Bannwarth and R. Mulhaupt, *J. Am. Chem. Soc.*, 2009, **131**, 8262; (f) Z. Jin, D. Nackashi, W. Lu, C. Kittrell and J. M. Tour, *Chem. Mater.*, 2010, **22**, 5695; (g) K. Jasuja, J. Linn, S. Melton and V. Berry, *J. Phys. Chem. Lett.*, 2010, **1**, 1853; (h) A. R. Siamaki, A. E. S. Khder, V. Abdelsayed, M. S. El-Shall and B. F. Gupton, *J. Catal.*, 2011, **279**, 1; (i) S. Moussa, V. Abdelsayed and M. S. El-Shall, *Chem. Phys. Lett.*, 2011, **510**, 179.

3. (a) Y. B. Liu, C. Khemtong and J. Hu, *Chem. Commun.*, 2004, 398; (b) T. Ishida and M. Haruta, *Angew. Chem. Int. Ed.*, 2007, **46**, 7154; (c) A. T. Gates, S. O. Fakayode, M. Lowry, G. M. Ganea, A. Murugeshu, J. W. Robinson, R. M. Strongin and I. M. Warner, *Langmuir*, 2008, **24**, 4107; (d) B. Deutsch, R. Hillenbrand and L. Novotny, *Nano Lett.*, 2010, **10**, 652; (e) I. A. Wani, S. Khatoon, A. Ganguly, J. Ahmed, A. K. Ganguli and T. Ahmad, *Mater. Res. Bull.*, 2010, **45**, 1033.

4. (a) S. Moussa, A. R. Siamaki, B. F. Gupton and M. S. El-Shall, *ACS Catal.*, 2012, **2**, 145; (b) K. Gotoh, T. Kinumoto, E. Fujii, A. Yamamoto, H. Hashimoto, T. Ohkubo, A. Itadani, Y. Kuroda and H. Ishida, *Carbon*, 2011, **49**, 1118; (c) Y. Z. Li, Y. Yu, J. G. Wang, J. Song, Q. Li, M. D. Dong and C. J. Liu, *Applied Catal. B: Environmental*, 2012, **125**, 189.

5. (a) A. Mastalir, Z. Kiraly, A. Patzko, I. Dekany and P. L'Argentiere, *Carbon*, 2008, **46**, 1631; (b) J. F. Shen, M. Shi, B. Yan, H. W. Ma, N. Li and M. X. Ye, *J. Mater. Chem.*, 2011, **21**, 7795; (c) A. Mastalir, Z. Kiraly, M. Benko and I. Dekany, *Catal. Lett.*, 2008, **124**, 34; (d) L. Ren, F. Yang, Y. F. Li, T. Liu, L. Q. Zhang, G. Q. Ning, Z. C. Liu, J. S. Gao and C. M. Xu, *RSC Adv.*, 2014, **4**, 26804.

6. (a) T. Kaneko, K. Baba, T. Harada and R. Hatakeyama, *Plasma Process. Polym.*, 2009, **6**, 713; (b) O. Hofft and F. Endres, *Phys. Chem. Chem. Phys.*, 2011, **13**, 13472.

7. B. J. Borah and D. K. Dutta, *J. Mol. Catal. A: Chem.*, 2013, **366**, 202.

8. (a) F. W. Zhang, J. Jin, X. Zhong, S. W. Li, J. R. Niu, R. Li and J. T. Ma, *Green Chem.*, 2011, **13**, 1238; (b) T. Mizutani, S. Honzawa, S. Tosaki and M. Shibasaki, *Angew. Chem. Int. Ed.*, 2002, **41**, 4680.

9. (a) T. Hashimoto, M. Tori and Y. Asakawa, *Phytochemistry*, 1988, **27**, 109; (b) D. J. Pope, A. P. Gilbert, D. J. Easter, R. P. Chan, J. C. Turner, S. Gottfried and D. V. Parke, *J. Pharm. Pharmacol.*, 1981, **33**, 297; (c) L. Ye, X. Y. Meng, X. M. Liu, J. H. Tang and Z. M. Li, *J. Appl. Polym. Sci.*, 2009, **111**, 2372.

10. (a) M. Gruber, S. Chouzier, K. Koehler and L. Djakovitch, *Appl. Catal. A: Gen.*, 2004, **265**, 161; (b) M. L. Kantam, R. Chakravarti, V. R. Chintareddy, B. Sreedhar and S. Bhargava, *Adv. Synth. Catal.*, 2008, **350**, 2544; (c) X. L. Fan, M. G. Manchon, K. Wilson, S. Tennison, A. Kozynchenko, A. A. Lapkin and P. K. Plucinski, *J. Catal.*, 2009, **267**, 114.

11. Z. Q. Tu, Z. C. Liu, Y. F. Li, F. Yang, L. Q. Zhang, Z. Zhao, C. M. Xu, S. F. Wu, H. W. Liu, H. T. Yang and P. Richard, *Carbon*, 2014, **73**, 252.

12. D. C. Marcano, D. V. Kosynkin, J. M. Berlin, A. Sinitskii, Z. Z. Sun, A. Slesarev, L. B. Alemany, W. Lu and J. M. Tour, *ACS Nano*, 2010, **4**, 4806.

13. (a) J. F. Shen, Y. Z. Hu, M. Shi, X. Lu, C. Qin, C. Li and M. X. Ye, *Chem. Mater.*, 2009, **21**, 3514; (b) R. Ramachandran, S. Felix, G. M. Joshi, B. P. C. Raghupathy, S. K. Jeong and A. N. Grace, *Mater. Res. Bull.*, 2013, **48**, 3834.

14. (a) L. M. Wei, F. Wu, D. W. Shi, C. C. Hu, X. L. Li, W. E. Yuan, J. Wang, J. Zhao, H. J. Geng, H. Wei, Y. Wang, N. T. Hu and Y. F. Zhang, *Sci. Rep.*, 2013, **3**, 9; (b) Q. S. Liu, K. K. Gath, J. C. Bauer, R. E. Schaak and J. H. Lunsford, *Catal. Lett.*, 2009, **132**, 342.

15. (a) Y. Zhao, G. S. Tang, Z. Z. Yu and J. S. Qi, *Carbon*, 2012, **50**, 3064; (b) C. H. Han, D. W. Hong, I. J. Kim, J. Gwak, S. D. Han and K. C. Singh, *Sens. Actuator B-Chem.*, 2007, **128**, 320.

16. M. Korzec, P. Bartczak, A. Niemczyk, J. Szade, M. Kapkowski, P. Zenderowska, K. Balin, J. Lelatko and J. Polanski, *J. Catal.*, 2014, **313**, 1.

RSC Advances Accepted Manuscript